METASTABLE EUTECTIC CONDENSATION IN A Mg-Fe-SiO-H₂-O₂ VAPOR: ANALOGS TO CIRCUMSTELLAR DUST

FRANS J. M. RIETMEIJER

Institute of Meteoritics, Department of Earth and Planetary Sciences, University of New Mexico, Albuquerque, NM 87131; fransjmr@unm.edu

JOSEPH A. NUTH III

Astrochemistry Branch, Code 691, NASA Goddard Space Flight Center, Greenbelt, MD 20771; uljan@lepvax.gsfc.nasa.gov

AND

JAMES M. KARNER

Department of Earth and Planetary Sciences, University of New Mexico, Albuquerque, NM 87131

ABSTRACT

Experimental studies of gas-to-solid condensation in a Fe-Mg-SiO-H₂-O₂ vapor reveal that this process yields only solids with magnesiosilica ($MgO.SiO_2$) and ferrosilica (Fe-oxide.SiO_2) compositions that coincide with metastable eutectics in the MgO-SiO_2 and (FeO/Fe_2O_3)-SiO_2 binary phase diagrams plus simple metal oxides (MgO, SiO_2, and FeO or Fe_2O_3). No solids form with mixed Mg-Fe-O compositions during condensation nor is there evidence for the formation of ferromagnesiosilica, $MgO.Fe_yO_x.SiO_2$ solids. The experimental evidence demonstrates that condensation of multicomponent vapors yields only a limited number of metastable solids of well-defined composition. These results have interesting consequences for models of grain formation in circumstellar outflows, for predictions concerning the chemical and mineralogical composition of presolar silicates, and for the composition of condensates formed in protostellar systems.

Subject headings: circumstellar matter — dust, extinction — ISM: abundances — molecular processes — solar system: formation

1. INTRODUCTION

Dust grains are observed to form in the winds of oxygen-rich asymptotic giant branch (AGB) stars, and it has been known for more than three decades that the infrared spectra of such materials are dominated by amorphous silicates (Woolf & Ney 1969). The exact nature of such condensates has been a matter of considerable debate owing to the broad nature of the dominant 10 and 20 μm features observed in most stellar sources and the difficulty of fitting such features with pure mineral components. Spectroscopic evidence obtained by the *Infrared Space Observatory* (*ISO*) has dramatically changed this situation (Waelkins et al. 1996; Waters et al. 1996) with the discovery of narrow emission features at longer wavelengths due to the presence of crystalline phases, i.e., silicate minerals.

Two different aspects of these observations are intriguing. First, the crystalline olivine and enstatite observed by *ISO* are nearly pure magnesium silicate grains. No evidence for the presence of iron-rich silicates has been obtained to date, and the observations indicate that the crystalline grains so far observed contain little, if any, iron. Second, observations of crystalline silicates have been confined to only the highest mass loss rate systems (Cami et al. 1998). In general, low mass loss rate stars produce only amorphous silicates. Even high mass loss rate systems produce primarily amorphous grains: less than ∼10% of the dust in such outflows is in the form of crystalline minerals (Tielens et al. 1998). In contrast to the expectation that more-crystalline materials would be observed in the highest temperature shells where thermal annealing could produce crystalline minerals from initially amorphous condensates, the observations indicate that almost the opposite could be true. Cooler shells appear to contain higher fractions of crystalline grains (Tielens et al. 1998).

Sogawa & Kozasa (1999) have demonstrated that it is possible to produce crystalline silicate grains in high mass loss rate AGB outflows by the heterogeneous condensation of silicate mantles onto previously condensed alumina cores followed by thermal annealing in the outflow. Their model cannot account for the production of nearly pure magnesium silicate minerals. Heterogeneous condensation of a magnesium-iron-silica vapor onto preexisting alumina surfaces should trap at least some of the iron that would then become incorporated into the crystalline silicate phases formed by annealing in the outflow. Similarly, Hallenbeck, Nuth, & Daukantes (1998) and Hallenbeck, Nuth, & Nelson (2000) have demonstrated that amorphous magnesium silicate grains anneal on much more rapid timescales than do amorphous iron silicates. However, until the experiments reported in this paper, there had been no reason to postulate the existence of separate populations of iron-rich and magnesium-rich silicates in a typical AGB outflow.

Theoretical studies of grain formation are ultimately based on the attainment of thermodynamic equilibrium and consider only the formation of stoichiometric crystalline silicate minerals as part of a fractional condensation sequence (Grossman & Larimer 1974; Lattimer & Grossman 1978; Gail 1998). Even models based on nucleation theory (e.g., Kozasa & Sogawa 1997; 1998) represent a judicious combination of kinetics and chemical thermodynamics. Previous vapor phase condensation experiments offered strong arguments against the likelihood of attaining equilibrium mineral assemblages even under controlled conditions in the terrestrial laboratory (e.g., De 1979; Donn 1979; Nuth 1996). Yet, equilibrium models remain central to our intuitive understanding of circumstellar dust formation.

To some extent this situation persists even more strongly in the meteoritics community. In the past, analytical techniques were unable to probe meteorites and experimentally produced dust analogs at the nanometer scale. Adequate analytical techniques are now available (Sutton 1994). Since 1974 March interplanetary dust particles (IDPs) have been routinely collected in the Earth's lower stratosphere (Brownlee, Tomandl, & Hodge 1976; Warren & Zolensky 1994). These particles are a new type of extraterrestrial material that is available for laboratory studies in addition to the meteorites (Mackinnon et al. 1982). The mineralogy and texture (Mackinnon & Rietmeijer 1987), and the high carbon (Thomas, Keller, & McKay 1996) and volatile element (Flynn et al. 1996) abundances, suggest that the IDPs are the least modified materials in the solar system. This zodiacal dust includes a sizeable fraction of debris from Oort cloud and Kuiper belt comets as well as dust from carbon- and ice-rich asteroids in the outer asteroid belt (Brownlee 1994). Such materials are our best hope of attaining a relatively unbiased sample of solids from the protosolar nebula.

2. PRINCIPAL COMPONENTS AND SYNTHETIC ANALOGS

Ultrafine-grained chondritic aggregate IDPs (5–25 μm in size) have a matrix with variable proportions of embedded Mg, Fe-olivine, (Ca, Mg, Fe)-pyroxene, Ni-free and low-Ni pyrrhotite, pentlandite, refractory Al,Ti-oxides, silicates and Fe-oxide grains, several micrometers in size (Rietmeijer 1998a). This matrix consists of three principal components (PCs) that are similar in size and composition to dust near the nucleus of comet Halley (Table 1). The carbon-free PCs are (1) coarse-grained smectite dehydroxylate, $(Mg, Fe)_6Si_8O_{22}$, units with $Fe/(Fe + Mg)$ (fe) = 0–0.36 (element ratio), and (2) ultrafine-grained units with a serpentine dehydroxylate, $(Mg, Fe)_3Si_2O_7$, composition and fe = 0.36–0.83. The minerals and texture of ultrafine-grained PCs are similar to the ferromagnesiosilica (Brownlee, Joswiak, & Bradley 1999) units of glass with embedded metals and sulfides (GEMS) (Bradley 1994; Bradley, Humecki, & Germani 1992). The chemical compositions of these PCs occur with rational atomic proportions but do not match the stoichiometric ratios of crystalline solids in which the three-dimensional arrangements of SiO_4 tetrahedra control the crystallochemical proportions of metals in the crystal lattice. The high degree of compositional order is one of the most remarkable properties of chondritic aggregate IDPs, but the origin of crystalline phases in these IDPs remains undetermined. Although the original dust accretion textures in these IDPs do not appear to have been significantly modified, such appearances might be deceiving. The observed properties of the PCs are the ultimate record of many possible processes: (1) aggregation of unaltered interstellar dust, (2) condensation in the solar nebula, (3) parent body alteration, (4) thermal modification of the dust during solar system sojourn, and (5) perihelion thermal processing in comet nuclei. Atmospheric entry flash-heating of IDPs may seriously modify their pre-entry properties, albeit in a recognizable manner (Rietmeijer 1996).

Given the current level of understanding of chondritic IDPs, ferromagnesiosilica PCs may represent surviving presolar dust that accreted 4.56 Gyrs ago. This dust experienced thermal modification at some time during its long history. Its main presolar characteristic is most likely to be its bulk composition rather than its mineralogy (Rietmeijer 1998a). Thus, the chemical composition of such dust may be the only constraint on the origin of this material. It is not evident whether originally amorphous ferromagnesiosilica

TABLE 1

PRINCIPAL COMPONENTS IN CHONDRITIC AGGREGATE IDPs[a] AND COMET P/HALLEY[b]

Principal Components in Chondritic Aggregate IDPs	Dust Particles in Comet P/Halley
Carbonaceous Units	
Refractory hydrocarbons and amorphous carbon units that are often fused in contiguous patches and clumps of vesicular, poorly graphitized and pregraphitic carbons. Units are 400–4000 nm in diameter.	CHON particles (carbon, hydrogen, oxygen, nitrogen)
Carbon-bearing, Ferromagnesiosilica Units	
Ultrafine (2 to ~50 nm) platy Fe,Mg-olivine, Mg, Fe-pyroxene, Fe, Ni-sulfide, iron oxide, and metallic iron in a refractory hydrocarbon and amorphous carbon matrix. The units contain minor Al, Ca, Cr, Mn and Ni, and traces of phosphorous and zinc. Units are ~100 nm in diameter.	"Mixed" particles (silicates plus carbon)
Ferromagnesiosilica Polyphase Units	
(1) Coarse-grained (10–410 nm) units that consist of Mg, Fe-olivine, Mg, Fe pyroxene and an amorphous Al-bearing silica material ±Ca,Mg and Fe. The units have a bimodal size distribution with mean diameters of 530 and 1140 nm, (2a) ultrafine-grained (<50 nm) units with an amorphous matrix containing Mg, Fe-olivine, Mg, Fe-pyroxene, Fe, Ni-sulfides and magnetite grains. Units are 125 nm to 1000 nm in diameter, and (2b) magnesiosilica units (100–1000 nm in diameter) of glass with embedded metal (kamacite) and sulfides.	Silicate [(Mg, Fe, Si)O] particles

NOTE.—The minerals in PCs are secondary phases that formed in situ in the amorphous units during flash heating when IDPs decelerate in the Earth's atmosphere between ~100–80 km altitude, parent body alteration, preaccretionary thermal processes (irradiation), or a combination of these processes.

[a] From Rietmeijer 1998a, and references therein.

[b] From Fomenkova et al. 1992.

FIG. 1. Transmission electron micrograph of magnetite in a Fe-Mg-SiO-H$_2$-O$_2$ condensed vapor. The diffraction maxima (*arrows*) in this orientation (*straight brackets*) confirm its single-crystal nature (*inset*). The gray background in all TEM images is the epoxy wherein the sample was embedded for ultramicrotome sectioning.

PCs are circumstellar condensates, materials condensed in the solar nebula or the result of thermal processing of circumstellar dust (Nuth, Hallenbeck, & Rietmeijer 1999a). Experimental studies can address this question by exploring the processes of dust formation and evolution through analog condensation and thermal annealing experiments (Hallenbeck et al. 1998; Nuth et al. 1999b) in the laboratory.

Circumstellar dust analogs produced in the laboratory by vapor-phase nucleation from Al-SiO-H$_2$-O$_2$, Mg-SiO-H$_2$-O$_2$ and Fe-SiO-H$_2$-O$_2$ vapors show several general properties:

1. Metal oxide-silica grains, ranging in size from mostly a few nanometers to 150 nm in diameter, form interconnected necklaces in fluffy smokes.

2. Grains in necklaces typically show evidence for surface free energy–driven coagulation and grain growth.

3. The fluffy texture offers restricted contact area for chemical exchange between the grains via solid state diffu-sion; the smokes are therefore chemically inactive during thermal annealing until their texture has collapsed at temperatures close to the melting point.

4. The grains include oxides with a stoichiometric mineral composition (Rietmeijer 1992) and nonstoichiometric mixed-metal oxide—SiO$_2$ grains.

5. Postcondensation autoannealing induces readjustments in condensed solids when the thermal energy of the grain is still high. Such reactions occur before condensed grains reach the quench temperature of the surrounding gas. The adjustments include homogeneous phase decomposition in nonstoichiometric mixed grains and crystallization of pure metal oxides.

6. Invariably, the individual, amorphous mixed metal-oxide/silica grains have well-defined composition distributions that match those of the metastable eutectics in the Al$_2$O$_3$-SiO$_2$ (Rietmeijer & Karner 1999), MgO-SiO$_2$ (Nuth et al. 1999b; Rietmeijer 1998b) and FeO/Fe$_2$O$_3$-SiO$_2$
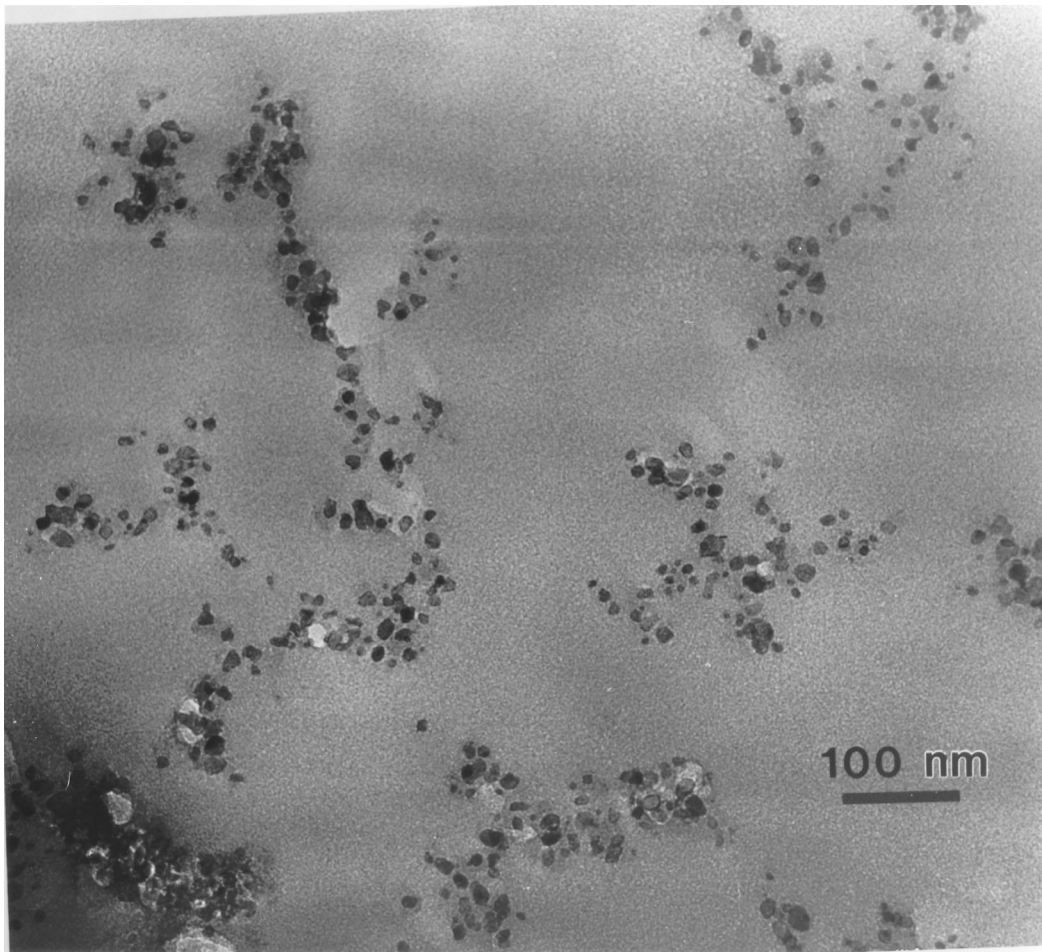
Fig. 2. Transmission electron micrograph of " FeSiO " necklaces in a condensed Fe-Mg-SiO-H_2-O_2 vapor.
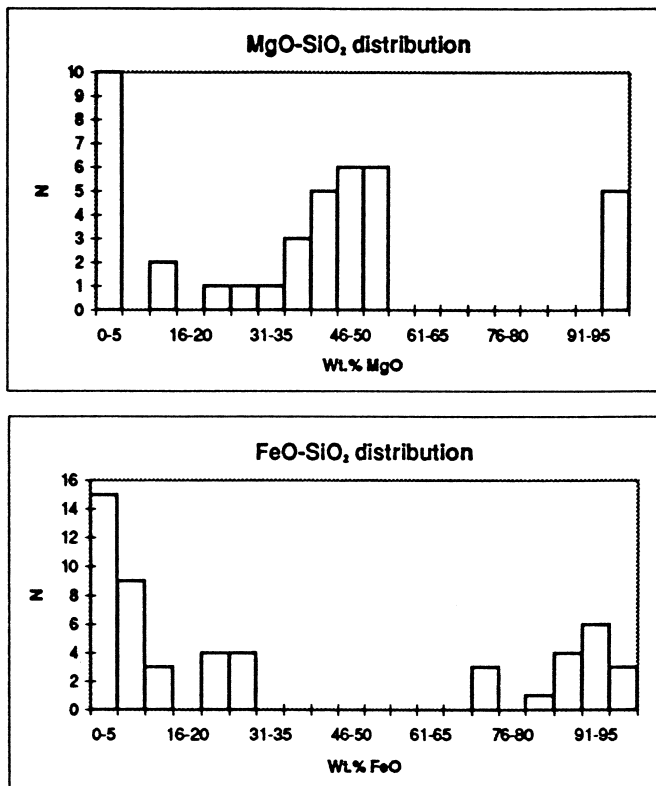
Fig. 3. Histograms of the distribution of individual solid grain compositions in a condensed Fe-Mg-SiO-H_2-O_2 smoke.

(Rietmeijer, Nuth, & Karner 1999) equilibrium phase diagrams.

Observation of both experimentally produced and natural condensation products that display metastable eutectic chemical compositions are the best proof yet that nonequilibrium vapor-phase condensation is not a chaotic event but rather proceeds to produce solids with predictable chemical order. The resulting amorphous solids resemble dissipative structures, states of organization wherein nonequilibrium becomes a source of order (Prigogine 1979). During nucleation in a cooling vapor, the first stable nuclei (molecules?) that form become seeds for grain growth when the remaining vapor condenses. Given sufficient activation energy and time, the condensed solids will arrange themselves into the least energetic physical and chemical configuration until they equilibrate with the ambient environment. However, kinetic factors might favor the formation of metastable high-energy states if the vapor condenses rapidly.

In this paper we report the results of a vapor-phase condensation experiment from a Fe-Mg-SiO-H_2-O_2 vapor. Instead of widely variable Mg/Fe/Si ratios scattered about the mean composition of the condensate we found only individual grains of compositionally ordered " MgSiO " and " FeSiO " solids in addition to pure end-member oxides. We predict that circumstellar outflows contain only a limited number of compositionally distinct condensed grain types with relative proportions that may vary among different
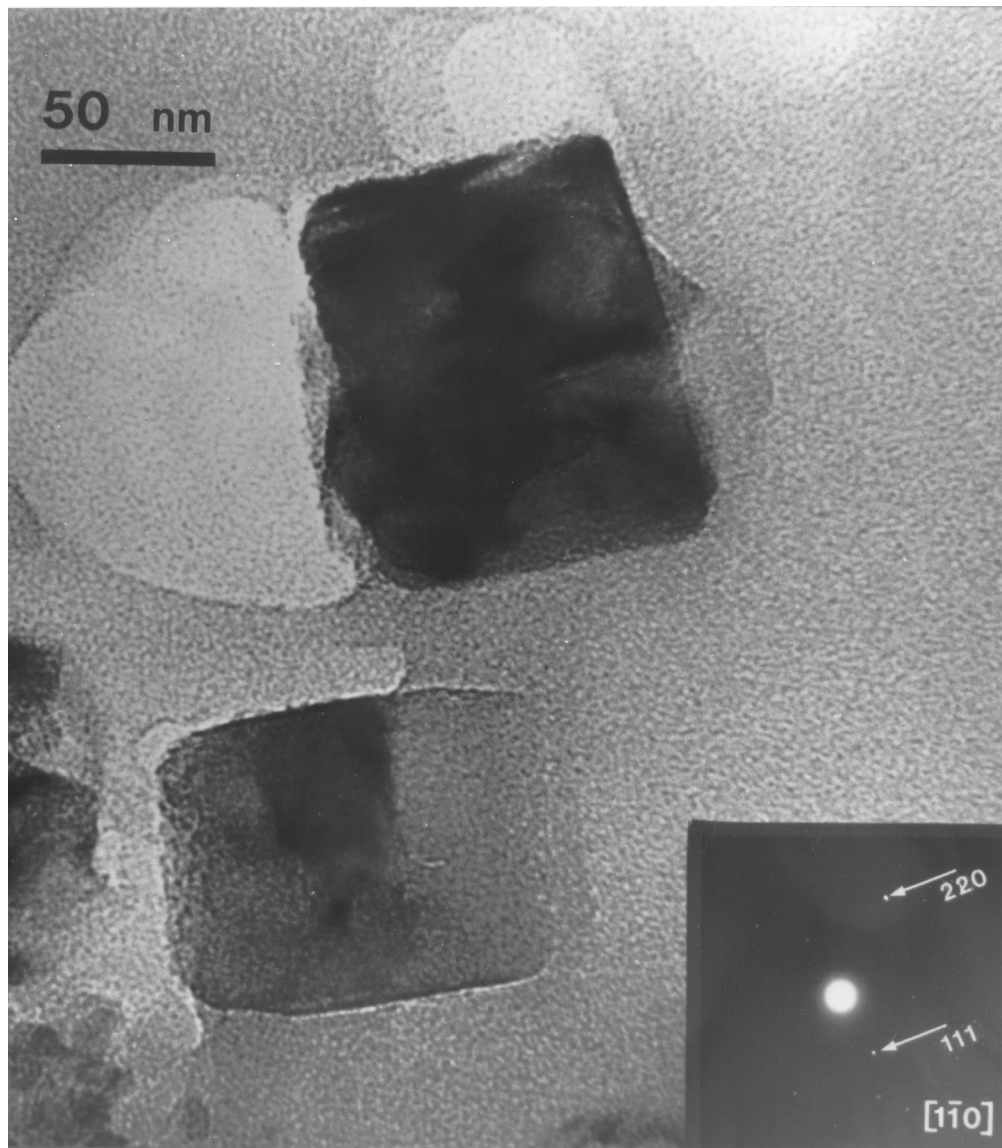
FIG. 4. Transmission electron micrograph of periclase (MgO) grains in a Fe-Mg-SiO-H$_2$-O$_2$ smoke. The diffraction maxima (*arrows*) in this orientation (*straight brackets*) confirm they are single crystals (*inset*).

stars. We submit that coarse-grained ferromagnesiosilica PCs in aggregate IDPs may be common circumstellar or protostellar condensates formed by postaccretion annealing of condensed dust aggregates.

3. EXPERIMENTAL PROCEDURE

The samples were produced by nonequilibrium gas-to-solid condensation in a Mg-Fe-SiO-H$_2$-O$_2$ vapor using the Condensation Flow Apparatus described by Nuth et al. (1988; 1999b). In this apparatus there is no standard set of flow, temperature, or pressure settings, but the following conditions are all at least somewhat typical of an average experiment. The total pressure in the system is ~ 100 torr, while the temperature in the furnace is ~ 1000 K. The hydrogen flow rate is ~ 1000 standard cubic centimeters per minute (sccm). The helium flow through the iron-carbonyl is on the order of 500 sccm. We estimate that the iron carbonyl concentration is $\sim 10\%$ of the total flow of helium. Magnesium metal is placed into a graphite boat inside the

furnace. At the nominal 1000 K temperature of the furnace, magnesium metal has a vapor pressure of ~ 5 torr. The oxygen flow rate always equals or exceeds that of silane (SiH$_4$) but is usually within a factor of 2 of the silane setting. The silane flow rate is typically ~ 100 sccm. As a result the hydrogen to oxygen ratio is always greater than 5, as some amount of hydrogen is also contributed by silane. The typical oxygen flow is sufficient to just balance the hydrogen contributed from the silane flow to produce water and Si^0 without effecting the bulk flow of hydrogen. In this system the oxygen fugacity during condensation is a dynamic quantity that is dependent on reaction rates, rather than a thermodynamic quantity. The actual oxygen fugacity during condensation is conducive to the formation of iron oxides instead of Fe^0, to the formation of silicon oxides instead of Si^0, and to the formation of magnesium oxides rather than to Mg^0. The exact bulk composition of the condensing gas is unknown but will be very close to the bulk composition of all solid grains in the resulting smoke. This composition can be obtained analytically (see below).
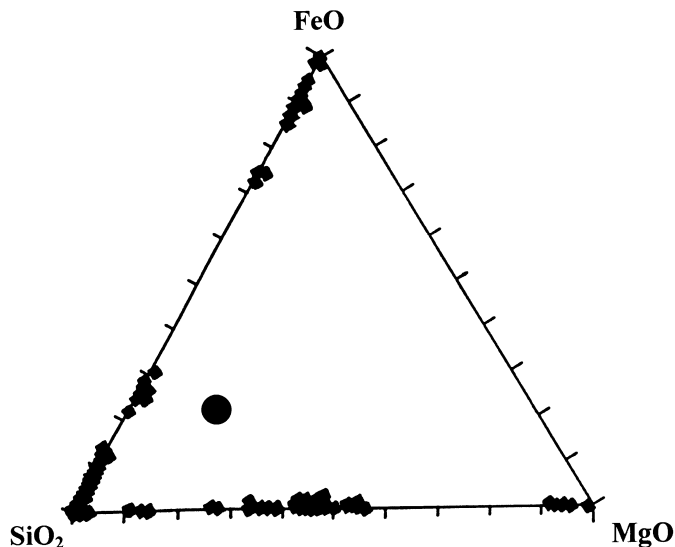
FIG. 5. Ternary diagram MgO-FeO-SiO$_2$ (oxide wt%) with the chemical compositions of gas to solid condensed solids from a Fe-Mg-SiO-H$_2$-O$_2$ vapor with metastable " MgSiO " and " FeSiO " solids matching the metastable eutectics. The "average bulk solid" composition (dot) is a proxy of the gas phase composition that was probably somewhat less SiO-rich.

Ultrathin sections of the smoke sample were prepared in a fashion similar to that employed in the analysis of IDPs (Bradley & Brownlee 1986). Mineralogical characterization of individual constituents in this smoke followed the same procedures used in studies of aggregate IDPs (Rietmeijer 1998a). The sample was analyzed by analytical and transmission electron microscopy (AEM, TEM) with a 0.2 nm spatial resolution in the TEM viewing mode and an analytical probe size of 10–20 nm in diameter for in situ determination of the chemical composition of individual grains greater than 10 nm in diameter. Rietmeijer & Karner (1999) provided details of the analytical procedures and data reduction techniques, and we refer the reader to this paper. Artifacts in grain compositions could arise from overlapping grains smaller than the section thickness (80–100 nm). This potential artifact was not a problem in this AEM study because the exact location of each chemical analysis was recorded on electron micrographs that were used to evaluate the possible "contamination" of individual analyses prior to data reduction. Also, prior to AEM analysis each grain was viewed using a "through-focus" technique to determine the presence of additional grains along the path of the analyzing electron beam. For the record we note that mineral alteration due to autoannealing following sample heating in the electron beam is readily recognizable (Rietmeijer et al. 1999) and did not effect our analyses.

4. RESULTS

Tridymite, a high-temperature silica polymorph, was observed to form spherical grains (~10 nm in diameter) that occur in aggregates and compact clusters up to ~200 nm in size. There is evidence for coarsening of these condensed grains to form ~30 nm-sized subhedral grains. These grains include Fe-bearing silica grains with up to 12 weight percent (wt%) FeO, or 11 wt% Fe$_2$O$_3$. Rare large (~165 nm in diameter) subspherical grains of amorphous silica were also found. Iron oxide grains (~34 nm in average diameter) are interspersed in the silica aggregates
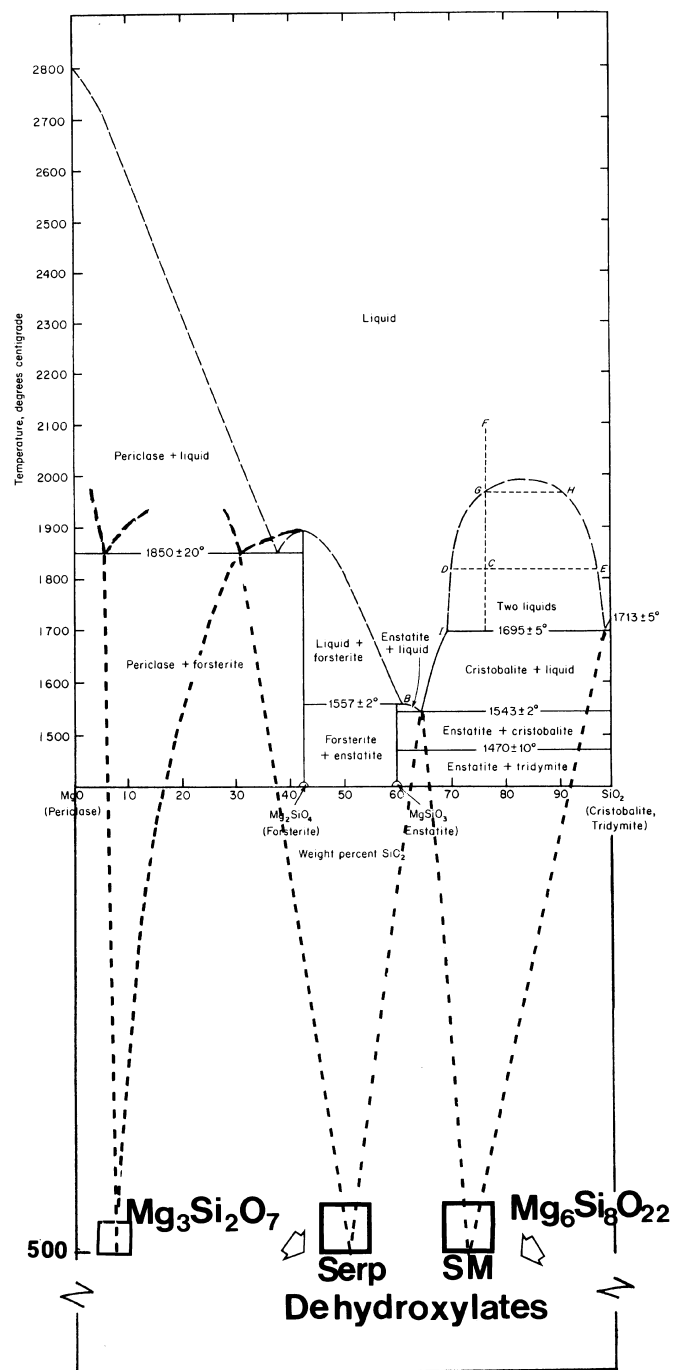
FIG. 6. MgO-SiO$_2$ phase diagram extended to the nominal quench temperature at 500° C with the observed metastable eutectic magnesiosilica grain compositions (open squares) for amorphous serpentine (serp) and smectite (SM) dehydroxylates and at ~85 wt% MgO.

and clusters. They are rounded single-crystal grains of magnetite (Fe$_3$O$_4$) or maghémite (γ-Fe$_2$O$_3$) up to ~350 nm in diameter with compositions that are ~85–100 wt% FeO (Fig. 1). Mixed "FeSiO" grains form both rounded and subhedral grains 10–30 nm in diameter (mean = 17 nm) arranged in strands (Fig. 2). They contain between 22–30 wt% FeO (mean = 26 wt% FeO), or 24–33 wt% Fe$_2$O$_3$ (Fig. 3). There is a hint of a fourth group of mixed FeSiO grains with compositions of between 70–75 wt% FeO. Rare periclase (MgO) crystals (90–100 wt% MgO) are observed to occur isolated from the remaining smoke material (Fig.

A FeO/Fe₂O₃ = 8/2

Two liquids
Cristobalite + liquid
Tridymite + liquid
Fayalite + liquid
Two liquids
Wüstite + liquid
Fayalite + wüstite
Fayalite + tridymite
Metastable eutectic
Greenalite dehydroxylate metastable eutectic
Metastable eutectic
Temperature, degree Centigrade
1800° 1600° 1400° 1200° 1000° 800° 600°
50   SiO₂

B FeO/Fe₂O₃ = 6/4

Two liquids
Cristobalite + liquid
Tridymite + liquid
Greenalite dehydroxylate + liquid
Greenalite dehydroxylate + tridymite
Fayalite + liquid
Two liquids
Magnetite + liquid
Fayalite + magnetite
Fayalite + greenalite dehydroxylate
Metastable eutectic
Greenalite dehydroxylate metastable eutectic
Metastable eutectic
$Fe_3Si_2O_7 + Fe_2SiO_4 = FMQ$
Temperature, degree Centigrade
1800° 1600° 1400° 1200° 1000° 800° 600°
50   SiO₂

FIG. 7. Revised FeO/Fe_2O_3–SiO_2 phase diagram at $FeO/Fe_2O_3 = 8/2$ (2A) and 6/4 (2B) showing the metastable eutectic points matching the observed ferrosilica compositions (*open squares*) produced by nonequilibrium gas to solid condensation. The positions of the high-silica eutectic point shifts as a function of variable FeO/Fe_2O_3. We made no attempt to control the oxygen fugacity, fO_2, during condensation but γ-Fe_2O_3 and Fe_3O_4 indicate oxidizing conditions, $fO_2 > 10^{-18}$ atm (500° C) and $fO_2 > 10^{-6}$ atm (1000° C) (see Lindsley 1976) A third metastable eutectic occurs as an iron serpentine dehydroxylate, $(Fe^{2+})_3Si_2O_7$. Its formation requires fO_2 values that promote FeO formation only. The condensed grains, 70–75 wt% FeO (see Fig. 5) in the Fe-Mg-SiO-H_2-O_2 vapor match this unique metastable eutectic. (Reproduced from Rietmeijer et al. 1999; copyright 1999 by the Royal Society of Chemistry.)

4). These sub- to euhedral grains range from 70 to 140 nm in size. Mixed "MgSiO" grains occur as clusters of rounded grains, 40–140 nm in diameter (mean = 78 nm), with an average of 43 wt% MgO. These listed compositions are averages of well-defined Gaussian populations of individual solid grains in this sample. The data summarized in the ternary diagram MgO-FeO-SiO_2 show: silica grains, MgO and Fe-oxide grains with limited solid solution of silica, and clusters of mixed "MgSiO" and "FeSiO" grains (Fig. 5). Note that there were no individual grains found in this sample with compositions on the "interior" of the ternary diagram and none that displayed the "average" composition of the original condensing vapor.

5. DISCUSSION

Gas-to-solid condensation in the Mg-Fe-SiO-H_2-O_2 vapor (Fig. 5) mimicked the condensation behavior observed separately in the MgO-SiO_2 and FeO/Fe_2O_3-SiO_2 systems: this is rather remarkable in that no mixed magnesium-iron silicate grains were observed at all. The grain morphology and size, mineralogy and compositional clusters of grains condensed in this Mg-Fe-SiO-H_2-O_2 vapor closely resemble those produced by condensation in the MgO-SiO_2 and FeO/Fe_2O_3-SiO_2 systems. Grains in the former had four peaks at ~0 wt% MgO (silica), at 28 wt% MgO, smectite dehydroxylate ($Mg_6Si_8O_{22}$), and 48

wt% MgO, serpentine dehydroxylate ($Mg_3Si_2O_7$), with Mg/(Mg + Si) (element) ratios of 0.4 and 0.55, respectively, and 95–100 wt% MgO (periclase) (Fig. 6). Four compositional peaks in the FeO/Fe_2O_3-SiO_2 system also occurred at 0, 15, 30, and 88 wt% FeO (Fig 7). These peaks match the metastable eutectic points and end member compositions in both equilibrium phase diagrams. The preferred metastable eutectic compositions are constrained by the liquidus topology of the MgO-SiO_2 and FeO/Fe_2O_3-SiO_2 phase diagrams. However, condensation in the ternary vapor did not produce any solids with preferred MgO-FeO/Fe_2O_3 compositions (Fig. 5), which suggests the absence of metastable eutectic points in the equilibrium phase diagram that would lead to the formation of this predictable phenomenon. Indeed, the phase relations in the MgO-Fe_2O_3 and MgO-FeO phase diagrams (Phillips, Somiya, & Muan 1961; Muan 1958) show complete magnesiowüstite [(Mg, Fe)O] or olivine [(Mg, Fe)$_2SiO_4$] solid solution at higher silica activity. There is no opportunity to form metastable eutectic solids of mixed Mg-Fe composition, which is consistent with the observations described here. We note that the Mg-Fe-Si oxide system has considerable cosmochemical interest because it describes not only the PC and chondritic IDP bulk compositions (Rietmeijer 1998a) but also the compositions of the meteorite matrix and of the fine-grained rims on chondrules in carbonaceous and
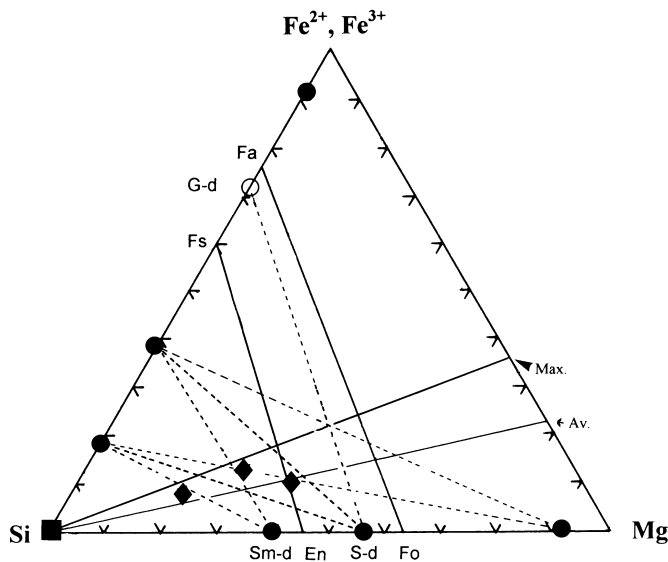
FIG. 8. Mg-Fe-Si (element wt%) diagram is used to compare major element compositions of IDPs, and matrix of undifferentiated carbonaceous and ordinary chondrites. Metastable cotectic-mixing lines (*dashed lines*) connect the compositions of the amorphous, metastable eutectic condensed solids (*dots*). These compositions are (1) smectite (Sm-d) and serpentine (S-d) dehydroxylates and two low-FeO smectite-like dehydroxylates (see Figs 6 and 7), (2) Si-bearing Fe- and Mg-oxides, and (3) silica grains (*solid square*). Fe^{2+}, Fe^{3+} symbolizes variations in the Fe^{2+}/Fe^{3+} ratios (legend to Fig. 7). Average *fe* (*Av.*; 0.23) and maximum (*Max.*) *fe* and three bulk compositions of these PCs (*filled diamonds*) are indicated. A metastable cotectic mixing line (*dashed lines*) connects the S-d and greenalite (G-d) (*open circle*) metastable eutectics. It is located in between the stoichiometric olivine (Fo-Fa) and pyroxene (En-Fs) lines.

unequilibrated ordinary chondrites (Zolensky & McSween 1988).

Our data support the hypothesis that nonequilibrium gas to solid condensation at considerable supercooling of a Fe-Mg-SiO-H_2-O_2 gas will produce amorphous grains with unique mixed "MgSiO" and "FeSiO" compositions defined by metastable eutectics, together with almost pure Si-oxide (tridymite), Fe-oxide (γ-Fe_2O_3) and Mg-oxide (periclase) (Fig. 8). The compositions of these mixed grains do not represent thermodynamic equilibrium that predicts stoichiometric pure Mg-silicates but not the formation of iron oxides. Instead iron is predicted to condense as metallic iron that will become oxidized when the temperature has fallen below $\sim 325°$ C. Equilibrium condensates in our experiment would have been magnesium silicates, iron metal, and free silica. Instead we find metastable eutectic magnesiosilica and ferrosilica condensates. Some of the simple metal oxides underwent a rapid, amorphous-to-crystalline transition without chemical readjustment by solid state diffusion, during autoannealing immediately after condensation and before thermal equilibration with the surrounding gas. The metastable nature of these grains was highlighted by the observation that thermal annealing of polycrystalline tridymite globules quickly brought about solid state amorphization. This transformation proceeded when amorphous silica nucleated at the surface and grain boundaries below the tridymite melting temperature but above its glass transition temperature (Rietmeijer et al. 1999). It appears that when sufficient energy is available to activate postcondensation modifications all of the condensed solids will ultimately exist as amorphous materials.

Condensation.—The finding that nonequilibrium gas-to-solid condensation of a Fe-Mg-SiO-H_2-O_2 vapor does not produce solids with mixed Mg/Fe/Si composition may be critical to understanding the nature of circumstellar dust. We submit that circumstellar dust grains originally condense as amorphous solids with predictable metastable eutectic "MgSiO" and "FeSiO" compositions plus a small fraction of metal oxide grains. Considering the cosmic abundances of the elements, these experiments indicate that the most common circumstellar condensates include only a limited number of compositionally well-defined grains. Because there are only a limited number of primary condensates, dust aggregates can form only along metastable cotectic mixing lines linking these primary metastable eutectics (Fig. 8). Postaccretion thermal annealing of simple, binary, or ternary MgO-FeO/Fe_2O_3-SiO_2 dust aggregates will produce mixed Mg-Fe-SiO_x grains, but these materials will still be compositionally unique solids.

Postcondensation modification.—Unique aggregate compositions are determined by the relative proportions of condensed dust grains on metastable cotectic mixing lines in the Mg-Fe-Si (element wt%) diagram (Fig. 8). The aggregate compositions along these mixing lines, and, more particularly, the compositions at the intersections of these lines, match the smectite dehydroxylate, $(Mg, Fe)_6Si_8O_{22}$, compositions of coarse-grained PCs in aggregate IDPs (Fig. 8). By virtue of their amorphous nature, the condensed dust contains a significant amount of internal, i.e., chemical (Clayton 1980), energy that can sustain spontaneous, kinetically controlled exothermic reactions of low activation energy. It seems likely that condensed dust aggregates will be able to undergo spontaneous exothermic reactions following some energetic event (grain collision, UV photon absorption) and become chemically homogeneous amorphous solids. The $fe = 0$–0.36 compositions of coarse-grained PCs are determined by the condensed "FeSiO" dust compositions and not by a "primary" solid solution mechanism established during condensation from the vapor. Such a mechanism is prohibited by the phase relationships in the MgO-Fe_2O_3 and MgO-FeO phase diagrams. During thermal annealing smectite dehydroxylate will undergo amorphous phase decomposition into serpentine dehydroxylate plus amorphous silica, viz., $(Mg, Fe)_6Si_8O_{22} \Rightarrow 2(Mg, Fe)_3Si_2O_7 + 4SiO_2$, whereby *fe* remains constant. Coarse-grained olivine [$(Mg, Fe)_2SiO_4$] and pyroxene [$(Mg, Fe)_2Si_2O_6$] (Fig. 9) with identical *fe* will form according to $2(Mg, Fe)_3Si_2O_7 \Rightarrow 2(Mg, Fe)_2SiO_4 + (Mg, Fe)_2Si_2O_6$, and will yield an olivine to pyroxene ratio of 2 to 1. Chemical analyses of the coarse-grained (10–410 nm) PCs in aggregate IDPs showed identical *fe* for the co-occurring olivine and pyroxene in each unit (Rietmeijer 1997). Although it is not clear when these minerals formed, flash heating simulation experiments (Joswiak & Brownlee 1998) suggest that they could form during deceleration of IDPs in the Earth's atmosphere. This point underscores our notion that the bulk composition of the ferromagnesiosilica units is the primary critical property of these grains when one looks for an explanation of their genesis. The minerals actually observed in collected aggregate IDPs could easily result from secondary alteration processes.

6. CONCLUSIONS

The gas-to-solid condensation experiments reported in this paper showed the formation of amorphous, mixed-
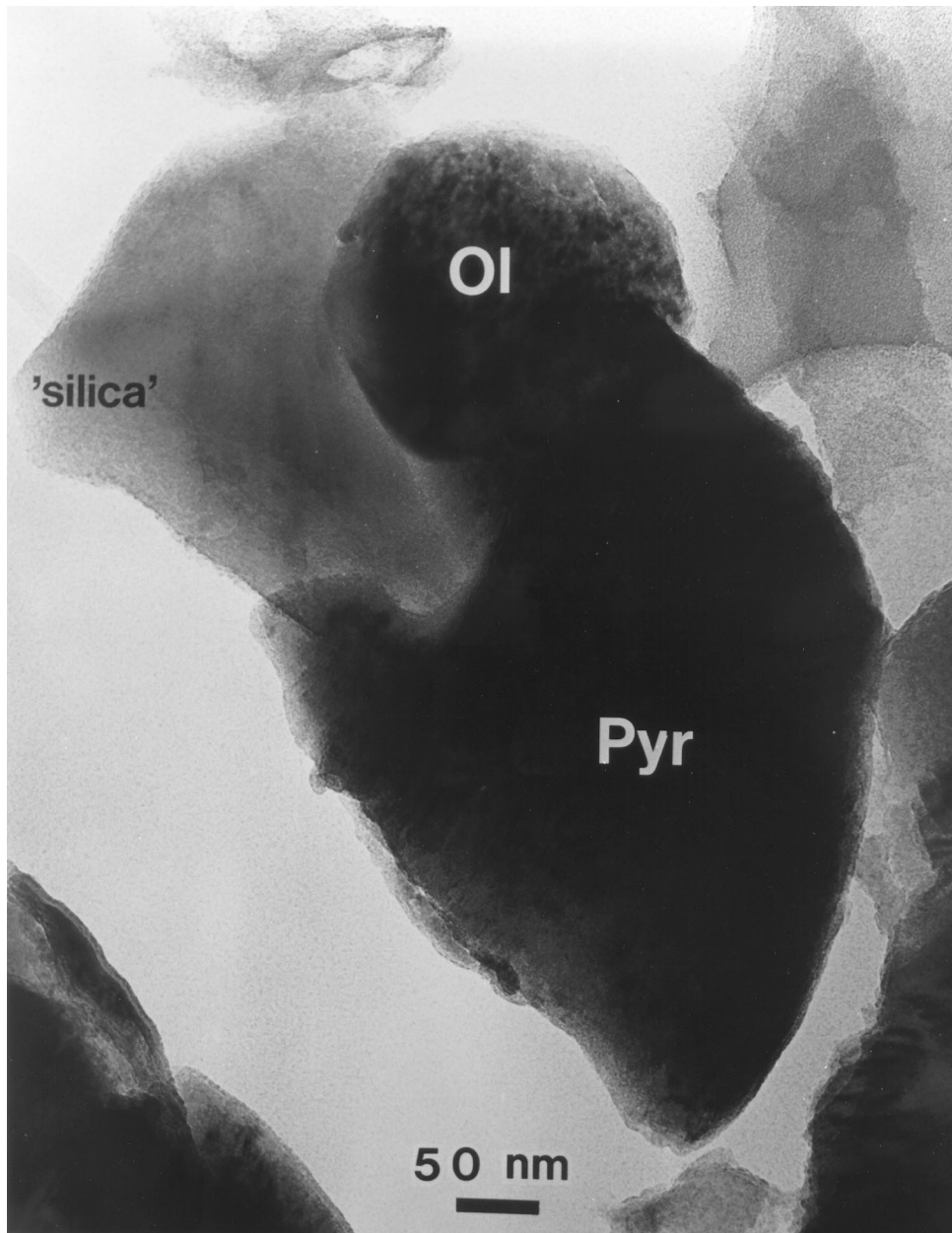
FIG. 9. Transmission electron micrograph of a coarse-grained ferromagnesiosilica PC in chondritic aggregate IDP L2011A9 showing the coexisting olivine (ol) and pyroxene (pyr) crystals along with an amorphous "silica" phase. After crystallization of the originally amorphous PC any Al and Ca that was present will reside in the nonstoichiometric "silica" phase (Reproduced from Rietmeijer 1998a, courtesy of the Mineralogical Society of America.)

oxide solids with predictable metastable eutectic compositions. These results imply that the composition of grains condensed in circumstellar outflows will include only solids with a very limited number of mixed "MgSiO" and "FeSiO" compositions. In particular, no mixed "MgFeSiO," i.e., ferromagnesiosilica, grains will form as primary condensates in such outflows. The experimental observations are consistent with *ISO* observations, indicating that the crystalline mineral fraction of high mass loss rate AGB dust consists almost exclusively of pure magnesium silicate minerals. No evidence of mixed "MgFeSiO" minerals has yet been observed. Our experimental results predict that no evidence for mixed "MgFeSiO" condensates will be found in such outflows.

Our experiments also have implications for the composition of grains formed via condensation in protostellar nebulae and, in particular, for the composition of primitive grains derived from comets in our own solar system, the aggregate IDPs. The coarse-grained, mixed oxide ferromagnesiosilica units in aggregate IDPs could not have formed directly by condensation but must have been formed following thermal processing of condensed dust aggregates. The high free energy of the metastable amorphous dust in the aggregates combined with the large surface free energy of nanometer-size grains probably facilitated formation of the compact amorphous units following the input of a small amount of "activation energy." There is no constraint on when this activation event might have occurred, and the minerals in the units in aggregate IDPs might therefore have formed during entry heating in the terrestrial atmosphere. The original aggregate compositions are defined by metastable cotectic mixing lines between the primary con-

densates. This again predicts that only limited variations in the chemical compositions of these nonchondritic units will be observed in aggregate IDPs and this prediction is consistent with the available observational evidence.

REFERENCES

Bradley, J. P. 1994, Science, 265, 925
Bradley, J. P., & Brownlee, D. E. 1986, Science, 231, 1542
Bradley, J. P., Humecki, H. J., & Germani, M. S. 1992, ApJ, 394, 643
Brownlee, D. E. 1994, in AIP Conf. Proc. 310, Analysis of Interplanetary Dust, ed. M. E. Zolensky, T. L. Wilson, F. J. M. Rietmeijer, & G. J. Flynn (New York: AIP), 5
Brownlee, D. E., Joswiak, D. J., & Bradley, J. P. 1999, Lunar and Planetary Science Conf. 30, CD-ROM, abstract 2031 (Houston: LPI)
Brownlee, D. E., Tomandl, D., & Hodge, P. W. 1976, in Interplanetary Dust and the Zodiacal Light, ed. H. Elsasser & H. Fechtig (New York: Springer:), 279
Cami, J., de Jong, T., Justtanont, K., Yamamura, I., & Waters, L. B. F. M. 1998, Ap&SS, 255, 339
Clayton, D. D. 1980, ApJ, 239, L37
De, B. R. 1979, Ap&SS, 65, 19
Donn, B. 1979, Ap&SS, 65, 167
Flynn, G. J. et al. 1996, in ASP Conf. Ser. 104, Physics, Chemistry and Dynamics of Interplanetary Dust, ed. B. A. S. Gustafson & M. S. Hanner (San Francisco: ASP), 291
Fomenkova, M. N., Kerridge, J. F., Marti, K., & McFadden, L.-A. 1992, Science, 258, 266
Gail, H.-P. 1998, A&A, 332, 1099
Grossman, L., & Larimer, J. W. 1974, Rev. Geophys. Space Phys., 1, 71
Hallenbeck, S. L., Nuth, J. A., III, & Daukantes, P. L. 1998, Icarus, 131, 198
Hallenbeck, S. L., Nuth, J. A., III, & Nelson, R. N. 2000, ApJ, in press
Joswiak, D. J., & Brownlee, D. E. 1998, Lunar and Planetary Science Conf. 29, CD-ROM, abstract 1929 (Houston: LPI)
Kozasa, T., & Sogawa, H. 1997, Ap&SS, 251, 165
———. 1998, Ap&SS, 255, 437
Lattimer, J. M., & Grossman, L. 1978, Moon Planets, 19, 169
Lindsley, D. H. 1976, in Oxide Minerals, ed. D. Rumble, III, (Washington, DC: Mineralogical Society of America), L-61
Mackinnon, I. D. R., McKay, D. S., Nace, G., & Isaacs, A. M. 1982, Proc. 13th Lunar Planet. Sci. Conf. (J. Geophys. Res. Suppl., No. 87, A413
Mackinnon, I. D. R., & Rietmeijer, F. J. M. 1987, Rev. Geophys., 25, 1527
Muan, A. 1958, Am. J. Sci., 256, 171
Nuth, J. A., III. 1996, in The Cosmic Dust Connection, ed. J. M. Greenberg (Dordrecht: Kluwer), 205
Nuth, J. A., III, Hallenbeck, S. L., & Rietmeijer, F. J. M. 1999a, Laboratory Studies of Silicate Smokes: Analog Studies of Circumstellar Materials. J, Geophys. Res., in press

Nuth, J. A., III, Hallenbeck, S. L., & Rietmeijer, F. J. M. 1999b, in Laboratory Astrophysics and Space Research, ed. P. Ehrenfreund, K. Krafft, H. Kochan, & V. Pironello (Dordrecht: Kluwer), 143
Nuth, J. A., III, Nelson, R. N., Moore, M., & Donn, B. 1988, in Experiments on Cosmic Dust Analogues, ed. E. Bussoletti, C. Fusco, & G. Longo (Dordrecht: Kluwer), 191
Phillips, B., Somiya, S. & Muan, A. 1961, J. Am. Ceram. Soc., 44, 167
Prigogine, I. 1979, Ap&SS, 65, 371
Rietmeijer, F. J. M. 1992, ApJ, 400, L39
———. 1996, Meteoritics Planet Sci., 31, 237
———. 1997, Lunar and Planetary Science Conf. 28, CD-ROM, abstract 1173 (Houston: LPI)
———. 1998a, in Planetary Materials, ed. J. J. Papike (Washington, DC: Mineralogical Society of America), 2-1
———. 1998b, Lunar. Planet. Sci. Conf. 29, CD-ROM abstract 1150 (Houston: LPI)
Rietmeijer, F. J. M., & Karner, J. M. 1999, J. Chem. Phys., 110, 4554
Rietmeijer, F. J. M., Nuth, J. A., III, & Karner, J. M. 1999, Phys. Chem. Chem. Phys., 1, 1511
Sogawa, H., & Kozasa, T. 1999, ApJ, 516, L33
Sutton, S. R. 1994, in AIP Conf. Proc. 310, Analysis of Interplanetary Dust, ed. M. E. Zolensky, T. L. Wilson, F. J. M. Rietmeijer, & G. J. Flynn (New York: AIP), 145
Thomas, K. L., Keller, L. P. & McKay, D. S. 1996, in ASP Conf. Ser. 104, Physics, Chemistry, and Dynamics of Interplanetary Dust, ed. B. A. S. Gustafson & M. S. Hanner (San Francisco: ASP), 283
Tielens, A. G. G. M., Waters, L. B. F. M., Molster, F. J., & Justtanont, K. 1998, Ap&SS, 255, 415
Waelkens, C., et al. 1996, A&A, 315, L245
Warren, J. & Zolensky, M. E. 1994, in AIP Conf. Proc. 310, Analysis of Interplanetary Dust, ed. M. E. Zolensky, T. L. Wilson, F. J. M. Rietmeijer & G. J. Flynn (New York: AIP), 245
Waters, L. B. F. M., et al. 1996, A&A, 315, L361
Woolf, N. J. & Ney, E. P. 1969, ApJ, 155, L181
Zolensky, M. E., & McSween, Jr., H. Y. 1988, in Meteorites and the Early Solar System, ed. J. F. Kerridge & M. S. Matthews (Tucson: Univ. Arizona Press), 114